Time-Resolved Polarized Fluorescence Spectroscopy Studies of Plasminogen Activator Inhibitor Type 1: Conformational Changes of the Reactive Center upon Interactions with Target Proteases, Vitronectin and Heparin†

Ming Fa,‡ Jan Karolin,§ Sergei Aleshkov,‡ Leif Strandberg,‡ Lennart B.-Å. Johansson,§ and Tor Ny*,‡

Departments of Medical Biochemistry and Biophysics and Physical Chemistry, Umeå University, S-90187 Umeå, Sweden

Received June 9, 1995; Revised Manuscript Received August 30, 1995⊗

ABSTRACT: Plasminogen activator inhibitor type 1 (PAI-1) is an important physiological inhibitor of the plasminogen activator system. To investigate the structure−functional aspects of this inhibitor, we have taken advantage of the lack of cysteine residues in the PAI-1 molecule and substituted Ser344 (P3) and Met347 (P1′), in the reactive center loop, with cysteines, thereby creating unique attachment sites for extrinsic fluorescent probe. Both cysteine mutants were purified and labeled with a sulfhydryl specific fluorophore, *N*-(4,4-difluoro-5,7-dimethyl-4-bora-3a,4a-diaza-*s*-indacenyl-3-propionyl)-*N*-(iodoacetyl)ethylenediamine (BDYIA). The labeled mutants were found to reveal biochemical characteristics very similar to those of wild type PAI-1. Time-resolved fluorescence spectroscopy was used to examine orientational freedom of BDYIA in the reactive center loop of PAI-1. The orientational freedom of the probe was found to be greater in the latent form than in the active form of PAI-1, suggesting that the reactive center has a more relaxed conformation in the latent form than in the active form. Complex formation with target proteases, tissue type plasminogen activator (tPA) and urokinase type plasminogen activator (uPA), caused decreased orientational freedom of BDYIA in the P3 position, while the orientational freedom of BDYIA in position P1′ increased to a level similar to that of BDYIA in reactive center-cleaved PAI-1. In contrast, complex formation with modified anhydro-uPA, which is unable to cleave its substrate, largely restricted the orientational freedom of BDYIA probe in the P1′ position. Together, these findings suggest that the P1−P1′ bond of the BDYIA-labeled PAI-1 mutants is cleaved in the native complex with PAs. Since vitronectin and heparin interact with PAI-1, their influence on the orientational freedom of BDYIA in the reactive center of the PAI-1 molecule was also studied. The fluorescence anisotropy suggests that interactions with vitronectin and heparin induce conformational changes in the reactive center, indicating that PAI-1 has a mobile reactive center loop which is conformationally linked to both the vitronectin and heparin binding sites.

The plasminogen activator (PA) system is responsible for the conversion of plasminogen to plasmin, thereby providing extracellular proteolysis in a variety of physiological processes (Saksela, 1985; Dano et al., 1985; Castellino, 1981; Bachmann, 1987; Moscatelli & Rifkin, 1988). The regulation of the PA system is complex and involves specific PA inhibitors that modulate the plasminogen activation (Saksela & Rifkin, 1988). Among these inhibitors, PA inhibitor type 1 (PAI-1)[1] is unique since it efficiently inhibits both the urokinase type PA (uPA) and tissue type PA (tPA) (Loskutoff et al., 1983; Chmielewska et al., 1988).

PAI-1 belongs to the serine protease inhibitor superfamily, commonly denoted as the serpin family (Carell & Travis, 1985). The serpins comprise structurally related proteins possessing a similar tertiary structure (Carrell & Boswell, 1986) and are likely to have evolved from a common ancestor. Like other serpins, the PAI-1 molecule has a reactive center located on a strained and exposed loop in the carboxyl terminal part of the molecule. Although the exact mechanism of inhibition is not known, the reactive center of PAI-1 is thought to act as a substrate with a "bait" P1 residue (Arg346) that mimics the normal substrate plasminogen (Carrell & Boswell, 1986).

The reactive center of PAI-1 can adapt varying conformations including active, latent, and substrate-like conformations (Hekman & Loskutoff, 1985; Declerck et al., 1988; Urano et al., 1992). The structures of the active PAI-1 molecule and its complex with PAs are not known, but it has been proposed that a mobile reactive loop is essential for the function of the inhibitor (Carrell et al., 1991). In the latent conformation, the reactive center region of PAI-1 is incorporated into the major β-sheet A (Mottonen et al., 1992), thereby resembling the structure of cleaved serpins (Bock, 1990). However, in contrast to cleaved serpins, only part of the reactive loop (P16−P4) is incorporated into sheet A

† This work was supported by the Swedish Natural Science Foundation, research Grants NFR BU 8473-308 and NFR Ku 8676-301.

* To whom correspondence should be addressed: Department of Medical Biochemistry and Biophysics, Umeå University, S-90187 Umeå, Sweden. Telephone: 46-90-166565. Fax: 46-90-136465.

‡ Department of Medical Biochemistry and Biophysics.

§ Department of Physical Chemistry.

⊗ Abstract published in *Advance ACS Abstracts,* October 15, 1995.

[1] Abbreviations: PAI-1, plasminogen activator inhibitor type 1; P3Cys, PAI-1 mutant S344C; P1′Cys, PAI-1 mutant M347C; tPA, tissue type plasminogen activator; uPA, urokinase type plasminogen activator; BDYIA, *N*-(4,4-difluoro-5,7-dimethyl-4-bora-3a,4a-diaza-*s*-indacenyl-3-propionyl)-*N*-(iodoacetyl)ethylenediamine; serpin, serine protease inhibitor superfamily; BODIPY, 4,4-difluoro-4-bora-3a,4a-diaza-*s*-indacene; NBD, 4-chloro-7-nitrobenzofurazan.

0006-2960/95/0434-13833$09.00/0

while the remaining residues (P2−P10′) are stretched along the surface of the protein.

PAI-1 associates with vitronectin in blood and in the extracellular matrix, which leads to a stabilization of the active conformation (Mimuro et al., 1987; Declerck et al., 1988; Wiman et al., 1988; Mimuro & Loskutoff, 1989; Wun et al., 1989). In addition, PAI-1, like several other serpins, interacts with heparin, leading to a substantial increase in PAI-1's efficiency to inhibit thrombin (Ehrlich et al., 1991). However, whether the binding of vitronectin or heparin influences the conformation of the reactive center remains to be determined.

Fluorescence spectroscopy can be applied for the detection of subtle changes in a protein structure (Dewey, 1991; Bastiaens et al., 1992), provided suitable fluorescent probes are incorporated at well-defined positions in the protein molecule. Recently, derivatives of BODIPY (4,4-difluoro-4-bora-3a,4a-diaza-*s*-indacene) such as *N*-(4,4-difluoro-5,7-dimethyl-4-bora-3a,4a-diaza-*s*-indacenyl-3-propionyl)-*N*-(iodoacetyl)ethylenediamine (BDYIA) have been spectroscopically characterized and found to be well-suited for fluorescence depolarization studies (Karolin et al., 1994).

In this study, we have analyzed BDYIA-labeled PAI-1 by means of polarized time-resolved fluorescence spectroscopy in order to monitor conformational changes in the reactive center that likely occur upon interactions with the target proteases and cofactors, such as vitronectin or heparin.

MATERIALS AND METHODS

Materials. The fluorescent-labeling reagent *N*-(4,4-difluoro-5,7-dimethyl-4-bora-3a,4a-diaza-*s*-indacenyl-3-propionyl)-*N*-(iodoacetyl)ethylenediamine (BDYIA) was obtained from Molecular Probes Inc. (Eugene, OR). Sephacryl S-200, heparin−agarose, and Sephadex G-25 were bought from Pharmacia AB (Uppsala, Sweden). The immobilized anhydrotrypsin was purchased from Pierce Chemical Co. (Rockford, IL). Heparin, *N*-acetyl-L-cysteine, dithiothreitol (DTT), and Tween 80 were from Sigma Chemical Co. (S Louis, MO). Ukidan (uPA) and Actilyse (tPA) were from Serono S. A. Aubonne (Switzerland) and Boehringer Ingelheim, International GmbH Ingelheim am Rhein (Germany), respectively. Single-chain and two-chain tPA (SC-tPA and tc-tPA, respectively) (activity standard) were from Biopool AB (Umeå, Sweden). The chromogenic substrates, S-2444 and S-2288, were purchased from Chromogenix AB (Mölndal, Sweden). The alkaline phosphatase-conjugated mouse antirabbit IgG(fc) was obtained from Promega-Biotech (Madison, WI). The purified human vitronectin was a generous gift from Dr. B. Wiman (Karolinska Institutet, Sweden).

Construction of Expression Plasmids for PAI-1 Cysteine Mutants. Single-stranded M13 DNA containing the PAI-1 cDNA (Lawrence et al., 1989) was used as a template for site-directed mutagenesis using a commercial *in vitro* mutagenesis kit (Amersham, U.K.). With the amino terminal valine of PAI-1 (Ny et al., 1986) designated as no. 1, residues Ser344 (P3) and Met347 (P1′) were substituted with cysteine. For the *in vitro* mutagenesis, oligomers 5′-CTGTCATAGTCTGTGCCCGCATG-3′ and 5′-CTCAGCCCGCTGTGCCCCCGAG-3′ were used. Nucleotides deviating from the wild type sequence are underlined. The identification and the subsequent cloning into a procaryotic experssion vector were performed as described earlier (Lawrence et al., 1989). The S344C and M347C mutants are denoted as P3Cys and P1′Cys, respectively.

Purification of the Wild Type and Mutant PAI-1 from Escherichia coli. The expression and purification of the wild type (wt PAI-1) and mutant PAI-1 were performed essentially as described (Lawrence et al., 1989). To ensure the removal of latent PAI-1 and the competence for the coupling of the fluorophore, the purified samples were finally loaded on a commercial anhydrotrypsin column (Pierce) equilibrated with the buffer containing 0.1 M NaCl and 0.15 M sodium phosphate of pH 6.6, washed with the same buffer, and eluted by 0.5 M Arg/HCl and 50 mM sodium phosphate of pH 6.6.

Labeling of the PAI-1 Cysteine Mutants with BDYIA. PAI-1 (10 μM), in 1.5 mL of buffer containing 50 mM sodium phosphate (pH 6.8), 0.5 M Arg/HCl, and 1 mM TCEP were labeled by the addition of BDYIA dissolved in 100% DMSO to a final concentration of 200 μM. The final concentration of DMSO in the labeling reaction was 3.6%. The reaction was performed in dark for 2 h at room temperature and then for 12 h at 4 °C. After the labeling reaction, an excess of BDYIA was removed by gel filtration on a Sephadex G-25 column equilibrated with a buffer containing 150 mM NaCl, 50 mM sodium phosphate (pH 5.6), and 0.01% Tween 80. The incorporation efficiency was calculated from the absorbances of BDYIA (λ_{max} = 505 nm) and PAI-1 (λ_{max} = 280 nm) by using the molar absorptivities of ϵ_{BDYIA} = 80 000 M^{-1} cm^{-1} and ϵ_{PAI-1} = 43 000 M^{-1} cm^{-1}.

Formation and Purification of Complexes between PAI-1 and PAs. About 0.4 mg of BDYIA-labeled PAI-1 mutant or wild type protein was mixed with uPA or two-chain tPA at a molar ratio of 1:1.2. The samples were then concentrated at 5000*g* with a microconcentrator (Amicon, Inc.) before the complexes were isolated on a Sephacryl S-200 molecular-sieving column equilibrated with a buffer containing 150 mM NaCl, 50 mM sodium phosphate (pH 5.6), and 0.01% Tween 80. Protein-containing fractions were analyzed by SDS−PAGE, followed by immunoblot analysis as described (Lawrence et al., 1989). Fractions containing purified complexes were pooled and either used directly or stored at −70 °C until use.

Preparation of Anhydro-uPA and Its Complex with PAI-1. Anhydro-uPA was prepared by the method described by Wun et al. (1989) except for the last step where the final product was not immobilized but dialyzed against 1 mM HCl and 0.2 M NaCl and subsequent with 0.2 M NaCl and 50 mM phosphate buffer (pH 5.6). The formation of anhydro-uPA/PAI-1 complex and their purification were performed as described for the above complex between PAI-1 and PAs.

Preparation of Reactive Center-Cleaved PAI-1 P1′Cys and Labeling with BDYIA. PAI-1 P1′Cys mutant (0.2 mg) was incubated with trypsin−sepharose (1.0 mg of trypsin) at room temperature for 10 min, after which the immobilized trypsin was removed by centrifugation. NH_2-terminal sequence analysis of the cleaved material revealed only two NH_2-terminal sequences corresponding to residues 1−5 and 347−351 of P1′Cys, indicating that the PAI-1 molecule was intact except for a specific cleavage of the P1−P1′ bond in the reactive center. The cleaved P1′Cys was labeled as described above.

Binding of Vitronectin and Heparin to PAI-1. To bind vitronectin and heparin to PAI-1, BDYIA-labeled PAI-1 was

mixed with vitronectin or heparin at a molar ratio of 1:1.2 and incubated at room temperature for 20 min. The amount of active PAI-1 bound to vitronectin was determined to be 45% as described previously (Lawrence et al., 1990).

Miscellaneous Methods for PAI-1. The assay used for PAI-1 inhibitory activity was performed as described (Lawrence et al., 1989). Kinetic analysis of the second-order rate constants for the interaction between the three forms of PAI-1 and single-chain tPA, two-chain tPA, and uPA were determined in a single-step assay as described (Lawrence et al., 1990). The rate of conversion from active to latent was determined as described earlier (Lawrence et al., 1990; Strandberg et al., 1991).

Fluorescence Spectroscopy. The steady state fluorescence spectra and anisotropies were obtained by using a SPEX Fluorolog 112 instrument (SPEX Industries, U.S.A.), equipped with Glan-Thompson polarizers. The temperature of the samples was kept at 5 ± 0.5 °C. The spectral band widths were 5.6 and 2.7 nm for the excitation and emission monochromators, respectively. The fluorescence spectra were corrected, and the fluorimeter was calibrated by using a standard lamp from the Swedish National Testing and Research Institute (Borås, Sweden).

A PRA 300 system (Photophysical Research Associates Inc., Ontario, Canada) was used for single-photon-counting measurements of the fluorescence decay. The excitation source is a thyratron-gated flash lamp (Model 510C, PRA) filled with deuterium gas and operated at about 30 kHz. The excitation wavelengths were selected by interference filters (Omega/Saven AB, Sweden) centered at 470 nm (HBW = 9.3 nm). The fluorescence emission was observed above 520 nm through a long pass filter (Schott, Germany). The maximum absorbance (at 505 nm) was kept below 0.08, corresponding to a BDYIA concentration of 1 μM.

The fluorescence decay curves were measured by repeated collection of photons during 200 s for each setting of the polarizers. The curves were deconvoluted on an IBM compatible PC by using a nonlinear least-square analysis based on the Levenberg−Marquardt algorithm. Typical results are shown in Figure 3. Further details are given elsewhere (Karolin et al., 1994).

Circular Dichroism Spectroscopy. The CD spectra of PAI-1 systems were recorded on a JASCO-J-720 spectrometer as described previously (Strandberg et al., 1991).

THEORETICAL PREREQUISITES

The fluorescence anisotropy, defined according to eq 1, is an orientational correlation function of excited fluorescent molecules.

$$r(t) = \frac{F_{ZZ}(t) - F_{ZX}(t)}{F_{ZZ}(t) + 2F_{ZX}(t)} \tag{1}$$

In eq 1, $F_{ZZ}(t)$ and $F_{ZX}(t)$ denote the intensities of fluorescence as a Z-polarized excitation light beam propagates along the laboratory X axis, while the emission is monitored along the Y axis, for the polarizer settings being parallel to the Z and X axes, respectively. The function $r(t)$ depends solely on the rotational motions and the local orientation of the fluorophores, provided that the excited state processes are independent of reorientational dynamics and provided that energy migration among the chromophores is negligible. Within these assumptions one obtains

$$r(t) = r_0 \sum_{m=-2}^{2} \langle D^{(2)}_{m0}(\Omega^0_{LM}) D^{(2)*}_{m0}(\Omega_{LM}) \rangle \tag{2}$$

Here, the orientational correlation functions given within the brackets are written in a basis of second-rank irreducible Wigner rotational matrices (Brink & Satchler, 1968). The orientations of a molecule at the time of excitation (*i.e.* $t = 0$), and at a time t later, are given by the eulerian angles of Ω^0_{LM} and Ω_{LM}. The subscript (LM) indicates that the angular transformation is from a laboratory-fixed (L) to a molecule-fixed (M) frame. The initial anisotropy $r_0 = {}^2/_5$, if the absorption and emission transition dipoles are parallel.

For a fluorescent molecule covalently linked to a globular protein molecule whose local mobility is independent of the overall rotation of the protein, it can be shown (Szabo, 1984) that

$$r(t) = r_0 \exp(-t/\phi_c) \sum_{m=-2}^{2} \langle D^{(2)}_{m0}(\Omega^0_{DM}) D^{(2)*}_{m0}(\Omega_{DM}) \rangle \tag{3}$$

Here, ϕ_c denotes the rotational correlation time of the protein molecule, and the expression within the brackets represents the local rotational correlation functions of the fluorophore. The r_0 value represents the limiting anisotropy of the fluorophore which is determined under conditions where the fluorophores undergo a negligible rotational motion on the time scale of fluorescence.

For the diffusive rotational motion of the protein, the correlation time is given by the Stokes−Einstein equation:

$$\phi_c = \frac{\eta V_h}{kT} \tag{4}$$

where η is the solvent viscosity, V_h is the hydrodynamic volume of the protein, and kT has its usual meaning (Cantor & Schimmel, 1980). A physical model is required for evaluating the correlation functions of eq 3. The detailed model should account for the restricted mobility of the probe in its site and the symmetry of the probe as well as the site, which is a task far from trivial. We will here assume that the local correlation function $\rho(t)$, can be written as

$$\rho(t) = \sum_k \rho_k \exp(-t/\Phi_k) + \rho_\infty \tag{5}$$

In eq 5, the Φ_k's are the effective rotational correlation times. The constant value of $r_0\rho_\infty$ corresponds to the residual fluorescence anisotropy, reached after sufficiently long times of $t \geq t_\infty$. The residual value of ρ_∞ can take values between 0 and 1, depending on the orientational distribution in the binding site. A cone model (Kinosita et al., 1977) is sometimes used as a simplifying orientational potential in anisotropic systems like membranes and proteins. It is then assumed that the probability of orientation of the transition dipole moment is the same for any angle less than the cone angle β_c. The cone angles reported in this work were calculated from

$$\rho_\infty = {}^1/_2 \cos\beta_c(1 + \cos\beta_c) \tag{6}$$

Table 1: Specific Inhibitory Activity of PAI-1 Cys Mutants against PAs before (−) and after (+) Labeling with BDYIA[a]

	wt PAI-1		P3Cys		P1′Cys	
	−	+	−	+	−	+
uPA	163	109	103.6	84.2	168	110
tPA	744	553	527	472	603	529

[a] Specific inhibitory activity was determined for untreated (−) and BDYIA-labeled (+) PAI-1 toward uPA (Ukidan) and tPA (Actilyse). Results are expressed as the international units of PA inhibited by 1 μg of PAI-1 (IU/μg). The specific activities of uPA and tPA were 142.5 and 601.5 IU/μg, respectively.

The angle β_c must of course not be taken literally. It merely serves as a rough estimate of the oriental restriction.

Note that the initial anisotropy

$$r(0) = r_0(\sum_k \rho_k + \rho_\infty) \quad (7)$$

For the case, one finds an initial anisotropy which is less than the limiting anisotropy, i.e. $r(0) < r_0$; rapid motions of the fluorophore take place on a time scale beyond the time resolution of the experiment. In the present study, rotational motions on the picosecond time scale or faster will give rise to such a deviation between $r(0)$ and r_0.

RESULTS AND DISCUSSION

Construction, Expression, and Purification of PAI-1 Cys Mutants. The reactive center loop (P17−P2′) of serpin is believed to be engaged in the process of inhibition (Huber & Carrell, 1989). To monitor conformational changes in the reactive center of PAI-1 during interactions with PAs and cofactors, we decided to use time-resolved fluorescence spectroscopy. For this purpose, unique attachment sites for sulfhydryl specific fluorophores were created in the reactive center loop by substitution of Ser344 and Met347 with cysteine residues. Referring to the positions of the substituted residues, the constructed mutants are denoted P3Cys and P1′Cys, respectively. The positions P3 and P1′ were chosen because they are located on opposite sides of the P1−P1′ bond and because previous studies have shown that P3 and P1′ can accept a variety of amino acids without affecting the inhibitory activity (York et al., 1991; Sherman et al., 1992).

Characterization of the PAI-1 Cys Mutants Labeled with BDYIA. The mutants were expressed in *E. coli*, and the proteins were purified to homogeneity. To test whether cysteine substitutions or the attachment of BDYIA to the reactive center affects the function of PAI, the specific inhibitory activity and second-order rate constants were determined before and after the labeling reaction. As shown in Table 1, the specific inhibitory activity of the two cysteine mutants before labeling was similar to that of wt PAI-1. The purified inhibitor mutants were labeled with the sulfhydryl specific fluorophore BDYIA as described in Materials and Methods. The degree of labeling was 85% for the P3Cys mutant, 70% for the P1′Cys, and less than 4% for wt PAI-1, indicating a sulfhydryl specific labeling of the mutants. The linkage between the sulfhydryl group and the fluorophore was found to be very stable, and labeling efficiency was not reduced following boiling in SDS (data not shown). As shown in Tables 1 and 2, P3Cys and P1′Cys maintain their function as inhibitors toward the PAs after the labeling. The specific inhibitory activity, as well as the second-order rate constants for the interaction of the PAI-1 cysteine mutants with PAs, was somewhat lower after labeling with BDYIA. However, the reduction was about the same for mutant and wt PAI-1, suggesting that it is due to the labeling reaction *per se* and not to the attachment of fluorophore.

Experiments were performed to test for complex formation between the BDYIA-labeled PAI-1 mutants and the PAs. As shown in Figure 1, the labeled cysteine mutants were equally efficient in forming complexes with uPA and the two-chain form of the tPA (tc-tPA) as wt PAI-1. Since PAI-1 can convert from an active to a latent form, we examined whether labeled PAI-1 mutants could adopt the latent conformation. As seen in Figure 2, both BDYIA-labeled P3Cys and P1′Cys were found to lose activity with an almost identical rate as wt PAI-1. The CD spectra of unlabeled and labeled PAI-1 Cys mutants were also determined and found to be almost identical to that of wt PAI-1 (data not shown). Together with the analysis described above, these data suggest that the labeled mutant inhibitors maintain a tertiary structure and function in a manner very similar to that of wt PAI-1.

Fluorescence Relaxation of BDYIA Attached to the P1′ and P3 Cys Residues. For both active P3Cys and P1′Cys, the fluorescence decays can be fit to a sum of two exponential functions. In all systems prepared with the buffer containing 150 mM NaCl, 50 mM sodium phosphate (pH 5.6), and 0.01% Tween 80 as the solvent, we found a dominating component (96%) connected with a fluorescence lifetime of $\tau_1 = 6.4 \pm 0.1$ ns and a smaller one with $\tau_2 = 1.8 \pm 0.7$ ns. The longer lifetime, τ_1, was significantly smaller in the systems prepared with a solvent mixture of buffer and glycerol (1:1 by volume). No significant changes of τ_1 and τ_2 were found in different regions of the fluorescence spectrum, revealing that the biexponentiality is not due to a slow environmental response to excited BDYIA. At present, we cannot give an unambiguous explanation to the biexponentiality (Karolin et al., 1994).

Table 3 summarizes the fluorescence lifetimes and the mean fluorescence lifetimes, $\langle\tau\rangle$, obtained for BDYIA in the P1′Cys and P3Cys mutants of active, latent, and cleaved PAI-1 and for PAI-1 in the presence of heparin or vitronectin, as well as in complex with the PAs. The variations of τ_1 and $\langle\tau\rangle$ are within 10%, while variations in τ_2 are somewhat larger. For the systems prepared with buffer−glycerol solutions, $\langle\tau\rangle$ was shorter but essentially constant. Taken together, the values of $\langle\tau\rangle$ are similar for all systems prepared with buffer, indicating that the photophysics of BDYIA is not sensitive to possible changes in the local structure.

Fluorescence Anisotropy of BDYIA in P1′ and P3 Cys Mutants. To analyze the time-resolved fluorescence anisotropy [$r(t)$], we have applied eqs 3−7. The rotational correlation time (ϕ_c) for PAI-1 was calculated to be 40 ns with eq 4 assuming a Stokes radius of 2.77 nm (Levin & Santell, 1987) and a solvent viscosity of $\eta = 1.69$ cP (at 277 K, Karolin et al., 1994). Values of $\phi_c > 20$ ns cannot be determined accurately with the actual lifetimes of $\langle\tau\rangle \approx 6$ ns. In the analysis of $r(t)$ with eqs 3 and 5, we have therefore used the estimated values of ϕ_c. The results obtained are given in the Tables 4−6.

In buffer, the steady state fluorescence anisotropy (r_s) of the probe in the latent form of PAI-1 was significantly lower than that of the active form (see Table 4). Since the

Table 2: Second-Order Rate Constants, k_1, for the Interactions between PAs and PAI-1 Cysteine Mutants before (−) and after (+) Labeling with BDYIA

	k_1 ($\times 10^7$ M^{-1} s^{-1})					
	wt PAI-1		P3Cys		P1′Cys	
	−	+	−	+	−	+
uPA	3.0 ± 0.6	1.5 ± 0.2	3.4 ± 0.5	1.8 ± 0.5	3.9 ± 1.0	2.0 ± 0.2
tc-tPA	4.3 ± 0.4	0.76 ± 0.02	6.3 ± 0.5	2.7 ± 0.1	4.5 ± 0.5	1.08 ± 0.01
sc-tPA	0.79 ± 0.02	0.45 ± 0.03	0.77 ± 0.05	0.45 ± 0.03	0.71 ± 0.05	0.24 ± 0.08

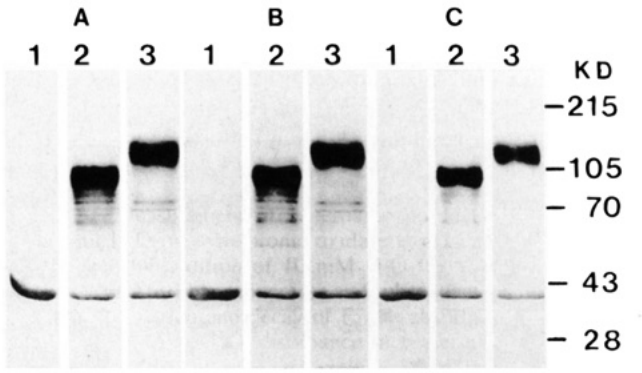

FIGURE 1: Immunoblot analysis of complexes formed between PA and PAI-1 or labeled Cys mutants of PAI-1. PAI-1 samples (0.2 mg) were incubated for 20 min alone or with equal molar amounts of uPA and two-chain tPA. After incubation, samples were separated by SDS−PAGE and examined by Western blot using rabbit antiserum against PAI-1: (A) wt PAI-1, (B) BDYIA-labeled P3Cys, and (C) BDYIA-labeled P1′Cys. In each panel the arrangement is as follows: (lane 1) PAI-1 only, (lane 2) PAI-1 with 0.25 mg of uPA, and (lane 3) PAI-1 with 0.3 mg of two-chain tPA. The molecular mass protein standards are indicated on the right.

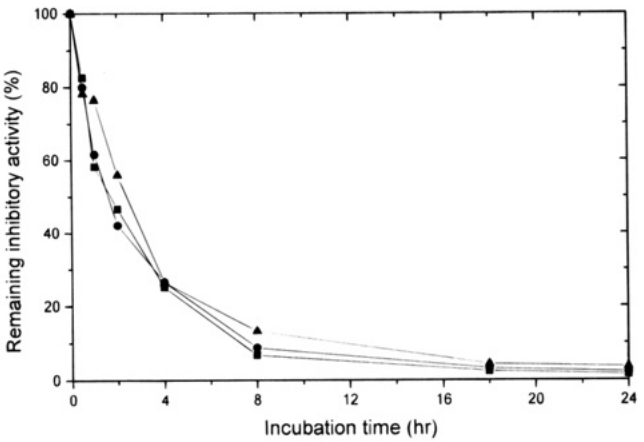

FIGURE 2: Stability of wt PAI-1 and BDYIA-labeled Cys mutants at 37 °C. PAI-1 samples (0.1 mg/mL) were dialyzed against 0.15 M NaCl and 50 mM phosphate buffer (pH 7.4) containing 0.5 mM dithiothreitol and 0.01% Tween 80. Following dialysis, the protein content and inhibitory activity against uPA was determined and assigned a value of 100%. Samples were then incubated at 37 °C, aliquots were removed at the times shown, and the specific activity against uPA was measured and compared with the starting value: (■) wt PAI-1, (●) BDYIA-labeled P3Cys, and (▲) BDYIA-labeled P1′Cys.

fluorescence relaxation was essentially the same (Table 3), it might at first be tempting to ascribe this lowering of the steady state anisotropy to larger contributions from rapid rotations of BDYIA in the latent forms. However, results extracted from the time-resolved fluorescence anisotropy (Table 4) reveal that the interpretation is more complex. The residual anisotropy values ($r_0\rho_\infty$) are lower in the latent forms,

Table 3: Fluorescence Relaxation[a] of BDYIA Bound to P1′Cys and P3Cys Mutants of PAI-1 under Different Conditions

system	τ_1 (ns)	f_1 (%)	τ_2 (ns)	f_2 (%)	$\langle\tau\rangle$	χ^2
P1′ active	6.2 ± 0.1	95.5	1.9 ± 0.7	4.5	6.0	0.94
P3 active	6.5 ± 0.1	96.2	1.7 ± 0.7	3.8	6.3	1.20
P1′ latent	6.4 ± 0.1	96.7	2.5 ± 1.2	3.3	6.3	0.93
P3 latent	6.6 ± 0.1	92.9	3.2 ± 0.7	7.1	6.3	1.03
P1′/uPA complex	6.0 ± 0.1	94.0	2.0 ± 0.6	6.0	5.8	0.99
P1′/tPA complex	6.2 ± 0.1	95.1	2.3 ± 1.0	4.9	6.0	1.01
P1′ cleaved	6.1 ± 0.1	85.1	3.1 ± 0.4	14.9	5.7	1.20
P1′/anhydro−uPA complex	5.9 ± 0.1	87.3	2.9 ± 0.4	12.7	5.5	1.06
P3/uPA complex	6.3 ± 0.1	95.5	2.4 ± 0.8	4.5	6.1	1.10
P3/tPA complex	6.0 ± 0.1	93.6	1.8 ± 0.6	6.4	5.7	1.01
P1′ + heparin	6.3 ± 0.1	94.3	1.9 ± 0.6	5.7	6.0	0.94
P1′ + vitronectin	6.3 ± 0.1	96.2	2.4 ± 1.1	3.8	6.2	1.07
P1′ in buffer-glyc[b]	5.5 ± 0.1	100			5.5	1.02
P3 in buffer-glyc	5.7 ± 0.1	95.0	1.5 ± 0.8	5.0	5.5	0.98
P1′ in buffer-glyc + hep[c]	5.5 ± 0.1	83.7	2.9 ± 0.3	6.3	5.5	0.99
P3 in buffer-glyc + hep	5.7 ± 0.1	90.2	2.6 ± 0.5	9.8	5.4	1.01

[a] The fluorescence decays were fit to $F(t) = a_1 \exp(-t/\tau_1) + a_2 \exp(-t/\tau_2)$; τ_1 and τ_2 are fluorescence lifetimes. The parameter χ^2 indicates the quality of the fit where values of 1.0 ± 0.2 are acceptable. The number f_i corresponds to the fraction of the total fluorescence intensity that is due to the lifetime of τ_i, that is, $f_i = (a_i\tau_i)(a_1\tau_1 + a_2\tau_2)^{-1}$. The average fluorescence lifetime $\langle\tau\rangle = f_1\tau_1 + f_2\tau_2$. [b] Buffer-glyc means buffer in 50% by volume of glycerol. [c] Heparin.

Table 4: Steady State (r_s) and Time-Resolved [$r(t)$] Fluorescence Anisotropy of BDYIA Bound to P1′ Cys and P3Cys Mutants of PAI-1 in Active and Latent Form[a]

		$r(t)$					
system	r_s	$r_0\varrho_1$	Φ_1 (ns)	$r_0\varrho_\infty$	$r_0\varrho_1 + r_0\varrho_\infty$	β_c (deg)	χ^2
P3 active	0.202	0.09	2.2 ± 0.9	0.205	0.295	35.8	0.87
P3 latent	0.192	0.10	3.3 ± 1.0	0.185	0.285	38.5	0.87
P1′ active	0.217	0.09	1.8 ± 0.7	0.226	0.316	33.0	1.06
P1′ latent	0.174	0.12	3.1 ± 0.7	0.154	0.274	42.8	1.18

[a] The time-resolved fluorescence anisotropy data were fit to eqs 3−6 using values of ϕ_c estimated from eq 4. For labeled P1′Cys and P3Cys mutants of PAI-1, ϕ_c = 40 ns. The parameter χ^2 indicates the quality of the fit where values of 1.0 ± 0.2 are acceptable.

as compared to the active forms, indicating that the orientational freedom of BDYIA is larger (β_c is increased) in the latent forms. The rotational correlation times (Φ_1) are slightly longer in the latent forms. It is expected that the pre-exponential factors [$r_0(\rho_1 + \rho_\infty)$] should be equal to r_0. However, a positive difference of $r_0[1 - (\rho_1 + \rho_\infty)]$ is obtained, compatible with an influence of rapid unresolved rotations (presumably on the picosecond time scale) in the latent as well as in the active form.

The time-resolved fluorescence anisotropy $r(t)$ for BDYIA in P1′ and P3 Cys mutants of active PAI-1 dissolved in a glycerol−buffer mixture (1:1 by volume) was also determined. Qualitatively, $r(t)$ varied in much the same way, as in buffer alone (Table 7). However, the rotational correlation time Φ_1 was about 3 times longer and the influence of rapid

Table 5: Steady State (r_s) and Time-Resolved [$r(t)$] Fluorescence Anisotropy of BDYIA Bound to P1′Cys and P3Cys Mutants of PAI-1 in Complex with PAs[a]

system	r_s	$r(t)$ $r_0\varrho_1$	Φ_1 (ns)	$r_0\varrho_\infty$	$r_0\varrho_1 + r_0\varrho_\infty$	β_c (deg)	χ^2
P3 active	0.202	0.09	2.2 ± 0.9	0.205	0.295	35.8	0.87
P3/uPA complex	0.318	0.03	2.6 ± 2.3	0.329	0.359	17.6	1.00
P3/tPA complex	0.326	0.03	8.1 ± 12	0.327	0.357	18.0	0.94
P1′ active	0.217	0.09	1.8 ± 0.7	0.226	0.316	33.0	1.06
P1′/uPA complex	0.186	0.07	2.9 ± 1.5	0.172	0.242	40.2	0.74
P1′/tPA complex	0.165	0.08	4.6 ± 1.9	0.134	0.214	45.6	1.02
P1′ cleaved	0.129	0.11	1.4 ± 0.6	0.117	0.227	48.2	0.96
P1′/anhydro-uPA	0.293	0.06	6.3 ± 3.4	0.276	0.336	26.1	1.01

[a] The time-resolved fluorescence anisotropy data were fit to eqs 3−6 using values of ϕ_c estimated from eq 4. For labeled P1′Cys and P3Cys mutants of PAI-1, $\phi_c = 40$ ns, and $\phi_c = 79$ and 90 ns for the complexes with uPA and tPA, respectively. The parameter χ^2 indicates the quality of the fit where values of 1.0 ± 0.2 are acceptable.

Table 6: Qualitative Effects on Orientational Freedom of BDYIA Attached to the P1′ and P3 Residues in Various Forms of PAI-1[a]

state of PAI-1	P1′	P3
native	–	–
latent	↑	↑
cleaved	↑↑	↑↑[b]
reacted with tPA	↑	↓↓
reacted with uPA	↑	↓↓
reacted with anhydro-uPA	↓↓	ND

[a] ↑ indicates increasing and ↓ decreasing orientational freedom of BDYIA, respectively. [b] Data not shown. [c] ND is not determined.

unresolved rotation was less, indicating that glycerol efficiently hampers the rotational rate of BDYIA in the PAI-1 molecule, while the residual anisotropy values $r_0\rho_\infty$ are close to those found in buffer. These data suggest that glycerol decreases rotational motions but does not perturb local structures in the P1′−P3 region of PAI-1.

As shown in Table 4, the analysis of the $r(t)$ reveals a significant difference for the BDYIA-labeled P1′ and P3 Cys mutants between the active and latent forms. For both positions, the residual anisotropies $r_0\rho_\infty$ are higher for BDYIA in the active form than in the latent form, meaning that the orientational freedom of the probe is more restricted (i.e. β_c is decreased) in the active form than in the latent form. This finding is compatible with the assumption that the reactive loop of serpins is stressed in the active form while it turns into a more relaxed and thermostable conformation after conversion to the latent form (Munch et al., 1991; Carrell & Evans, 1992). Consistent with these findings, the structure of latent PAI-1 (Mottonen et al., 1992) reveals that only part of the reactive loop (P16−P4) is incorporated into sheet A while the remainder (P2−P10′) forms an extended loop which is stretched along the surface of the protein.

Conformational Changes in the Reactive Center following Complex Formation with PAs. Little structural information is available in the literature for serpins complexed to serine proteases, and the mechanism by which these large inhibitors interact with their target proteases is not fully known. The nature of the interaction between the P1−P1′ peptide bond and the protease has been the subject of dispute (Gettins et al., 1993). Serpins may be cleaved at the reactive center residue like what has been formed for small protease inhibitors (Bode & Huber, 1991). Consistent with this proposal, C1 inhibitor expresses a neoepitode in complex with kallikrein that is also present in cleaved C1 inhibitor (de Agostini et al., 1988). In SDS−PAGE, serpin protease complexes migrate as higher molecular mass bands that represent serpin/protease adducts that involve an acyl−ester linkage between the P1 residue of a cleaved serpin and the active site serine of the proteinase. However, the demonstration of cleavage and acyl−ester formation under denaturing conditions do not prove that such an intermediate exists in the native serpin/protease complex, since denaturation may alter the stability of a noncleaved complex and push the interaction toward cleavage. In agreement with this, ^{13}C-NMR spectroscopy of the complex between human α_1-proteinase inhibitor and porcine pancreatic elastase involves a tetrahedral intermediate at P1 carbonyl and not an acyl intermediate (Matheson et al., 1991). This intermediate was stable during several days of incubation, suggesting that the formation of modified inhibitor cleaved in the reactive center proceeds very slowly. The complexes between α_2-antiplasmin and trypsin or chymotrypsin can also dissociate to give active inhibitor and protease, suggesting that the serpin/protease complexes are trapped at a stage before cleavage (Shieh et al., 1989). To study the influence of tPA and uPA on the conformation of the reactive center of PAI-1, complexes between BDYIA-labeled PAI-1 Cys mutants and PAs were analyzed. We routinely analyzed the complex samples before and after the fluorescence measurement. As we previously observed for NBD-labeled complexes (Strandberg et al., 1994), these complexes were found to be extremely stable and no dissociation could be detected during the experimental procedures (data not shown). As shown in Table 5, complex formation with PAs caused dramatic but divergent effects on the orientational freedom of BDYIA in position P3 and P1′. For BDYIA in position P3, complex formation with both tPA and uPA resulted in less influence from rapid unresolved motions as judged from the increased value of $r_0\rho_1 + r_0\rho_\infty$. The residual anisotropy ($r_0\rho_\infty$) increased and the cone angle (β_c) decreased following complex formation with PAs, which showed that orientational freedom of BDYIA was restricted. In contrast, when BDYIA was attached to P1′Cys, the orientational freedom was released (Figure 4B) and the contribution of rapid unresolved motion increased after complex formation. The restriction of the local orientational freedom of BDYIA in P3 is expected since PAI-1 interacts with PAs through its reactive center loop and this interaction is likely to involve the P3 residue. The increased orientational freedom of BDYIA in P1′ was not expected and suggests that a dramatic structural rearrangement of the reactive center loop takes place following the interaction with PAs.

The increased local orientational freedom of the BDYIA probe attached to P1′ following complex formation could be caused by a cleavage of the P1−P1′ peptide bond. We therefore investigated the orientational freedom of BDYIA attached to P1′ in PAI-1 where the P1−P1′ peptide bond had been cleaved. As shown in Table 5, the orientational freedom as well as the rapid unresolved motion were similar in BDYIA-labeled cleaved P1′Cys to that of BDYIA-labeled P1′Cys in complex with PAs. To further test the hypothesis that PAI-1 is cleaved in complex with PAs, the complex between BDYIA-labeled P1′Cys and catalytically inactive anhydro-uPA was formed. As shown in Table 5, the orientational freedom of the probe in P1′, as judged from the residual anisotropy as well as the influence of rapid unresolved motions, became more restricted following

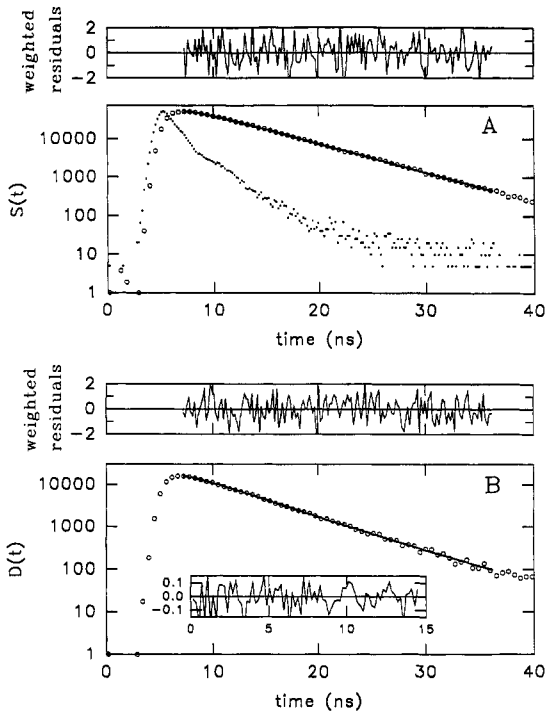

FIGURE 3: (A) Fluorescence relaxation or sum curve $S(t)$ and (B) difference curve $D(t)$ of BDYIA in the P1′Cys mutant of PAI-1 in glycerol buffer (50:50 by volume). The dotted curve in part A is the response function. In part B, the autocorrelation of the fit is inserted. The temperature is 278 K.

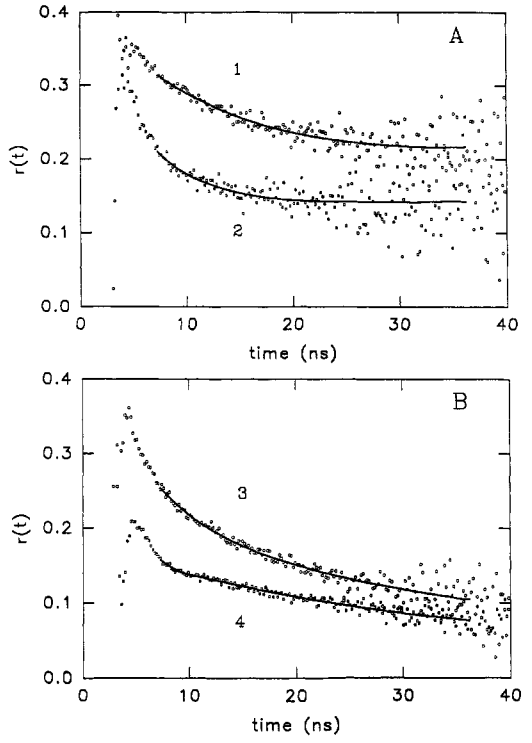

FIGURE 4: (A) Time-resolved fluorescence anisotropy, $r(t)$, of BDYIA in the P1′Cys mutant of PAI-1 in the absence (curve 1) and presence (curve 2) of heparin. The solution is a mixture of water buffer and glycerol (50:50 by volume). (B) Time-resolved fluorescence anisotropy, $r(t)$, of BDYIA in P1′Cys mutant of PAI-1 (curve 3) and its complex with tPA (curve 4) in buffer. The temperature is 278 K.

complex formation with anhydro-uPA, revealing a similar pattern as found for the probe in position P3 in complex with active PAs. Together, these experiments indicate that

Table 7: Steady State (r_s) and Time-Resolved [$r(t)$] Fluorescence Anisotropy of BDYIA Bound to P1′Cys and P3Cys Mutants of PAI-1 in the Reactions with Vitronectin and Heparin[a]

system	r_s	$r(t)$ $r_0\varrho_1$	Φ_1 (ns)	$r_0\varrho_\infty$	$r_0\varrho_1 + r_0\varrho_\infty$	β (deg)	χ^2
P3 active	0.202	0.09	2.2 ± 0.9	0.205	0.295	35.8	0.87
P3 + vitronectin	0.201	0.10	5.4 ± 2.1	0.160	0.260	41.9	1.18
P3 + heparin	0.192	0.07	3.4 ± 1.8	0.191	0.261	37.7	1.03
P3 in buffer-glyc[b]	0.274	0.15	7.0 ± 1.3	0.192	0.342	37.5	1.17
P3 in buffer-glyc + hep[c]	0.184	0.06	3.7 ± 2.6	0.160	0.220	41.9	1.11
P1′ active	0.217	0.09	1.8 ± 0.7	0.226	0.316	33.0	1.06
P1′ + vitronectin	0.220	0.11	7.5 ± 2.6	0.154	0.264	42.8	0.99
P1′ + heparin	0.211	0.10	3.1 ± 1.5	0.185	0.285	38.4	0.93
P1′ in buffer-glyc	0.286	0.13	6.6 ± 1.6	0.217	0.347	34.2	0.89
P1′ in buffer-glyc + hep	0.189	0.12	2.7 ± 0.9	0.144	0.264	44.2	0.95

[a] The time-resolved fluorescence anisotropy data were fit to eqs 3−6 using values of ϕ_c estimated from eq 4. For labeld P1′Cys and P3Cys mutants of PAI-1 in normal buffer, $\phi_c = 40$ ns. In glycerol, $\phi_c \rightarrow \infty$ on the time scale of fluorescence. The parameter χ^2 indicates the quality of the fit where values of 1.0 ± 0.2 are acceptable. [b] Buffer-glyc means buffer in 50% by volume of glycerol. [c] Heparin.

the BDYIA-labeled PAI-1 Cys mutants are cleaved in the complex with PAs, suggesting that the complex is trapped at the stage of an acyl−enzyme intermediate.[2] Our results are consistent with the recent observation that complex formation between PAI-1 labeled with NBD at position P9 and PAs leads to an increased fluorescence and a blue spectral shift similar to that observed for elastase-cleaved PAI-1 (Shore et al., 1995). Table 6 summarized the qualitative effects of the various manipulations on the orientational freedom of the probe at both positions in the PAI-1 molecule.

Fluorescence Anisotropy of BDYIA in P1′ and P3 Cysteine Mutants in the Presence of Vitronectin and Heparin. Vitronectin and heparin both bind to PAI-1, and these interactions lead to functional alterations of the inhibitor (Declerck et al., 1988; Wiman et al., 1988; Mimuro & Loskutoff, 1989; Ehrlich et al., 1991). In plasma, as well as in the growth substratum, PAI-1 is associated with vitronectin which results in a stabilization of the active conformation (Declerck et al., 1988; Wun et al., 1989). In the presence of heparin, the specificity of PAI-1 toward thrombin is substantially increased, suggesting that heparin may induce conformational change of the PAI-1 molecule. To establish whether interactions with vitronectin and heparin affect the conformation of the reactive center, we examined the time-resolved fluorescence anisotropy of BDYIA attached to P3Cys and P1′Cys in the absence and presence of vitronectin and heparin. For both P3Cys and P1′Cys labeled with BDYIA, addition of vitronectin caused a considerable decrease of the residual anisotropy as well as an increased influence of unresolved rapid motion (Table 7). These data indicate that the orientational freedom of the probes increases in the presence of vitronectin, suggesting that the binding of vitronectin induces conformational changes of the PAI-1 reactive center.

[2] Note Added in Proof: Recently, we (Wilczynska, Fa, Ohlsson, and Ny) and others (D. Lawrence, personal communication) have performed NH_2-terminal sequence analysis of chemically modified native serpin/protease complexes. These analyses have revealed that PAI-1 as well as two other serpins are cleaved in the native complex with their cognate proteases.

Also, addition of heparin affects the fluorescence anisotropy of BDYIA attached to P3 and P1′ cysteine residues of PAI-1 (see Figure 4A). Small changes of $r(t)$ for both BDYIA-labeled P3Cys and P1′Cys are seen following the addition of heparin (Table 7). However, the difference became more evident when the experiments were carried out in the solutions containing 50% of glycerol. Heparin appears to significantly increase the orientational freedom of BDYIA as well as increase the influence of very rapid reorientational motion. These results indicate that a conformational change of the reactive center region of PAI-1 takes place following the interaction with heparin. Since our fluorescence anisotropy measurements reveal that orientational freedom of the probe increases in the presence of heparin, it is possible that the reactive center of PAI-1 becomes more accessible to certain proteases after the binding of heparin which may be a reason for the increased efficiency to inhibit thrombin (Ehrlich et al., 1991). Heparin also binds to antithrombin III, thereby causing a dramatic increased association rate with target proteases (Rosenberg & Damus, 1973). Consistent with our finding on PAI-1, it was recently found that heparin induces conformational change in the antithrombin III molecule (Dawes et al., 1994). The nature of the conformation change that takes place following the binding of heparin to PAI-1 and antithrombin III remains to be clarified. Together with data on antithrombin III (Dawes et al., 1994), our data on PAI-1 support the concept that heparin binding sites in serpins are conformationally linked to mobile reactive centers.

ACKNOWLEDGMENT

We thank Mrs. Eva Vikström for her skillful technical assistance. We also express our gratitude to Dr. Björn Wiman (Department of Clinical Chemistry, Karolinska Hospital, Sweden) for his generous gift of purified human vitronectin and Dr. Robin W. Carrell (University of Cambridge, U.K.) for valuable discussions and advice.

REFERENCES

Bachmann, F. (1987) in *Thrombosis and Haemostasis* (Verstaete, M., Vermylen, L., Lijnen, R., & Arnout, J., Eds.) pp 227−266, Leuven University Press, Leuven, Belgium.

Bastiaens, P. I. H., van Hoek, A., Wolkers, W. F., Brochon, J.-C., & Visser, A. J. W. G. (1992) *Biochemistry 31*, 7050−7060.

Bock, S. C. (1990) *Protein Eng. 4*, 107−108.

Bode, W., & Huber, R. (1991) *Curr. Opin. Struct. Biol. 1*, 45−52.

Brinck, D. M., & Satchler, G. R. (1968) *Angular Moment*, Oxford University Press, Oxford.

Cantor, C. R., & Schimmel, P. R. (1980) in *Biophysical chemistry, Part II* (Freeman, H., Ed.) San Francisco, CA.

Carell, R., & Travis, J. (1985) *Trends Biochem. Sci. 10*, 20−24.

Carrell, R. W., & Boswell, D. R. (1986) in *Proteinase Inhibitors* (Barret, A., & Salvesen, G., Ed.) Elsevier, Amsterdam.

Carrell, R. W., & Evans, D. L. I. (1992) *Curr. Opin. Struct. Biol. 2*, 438−446.

Carrell, R. W., Evans, D. L., & Stein, P. E. (1991) *Nature 353*, 576−578.

Castellino, F. J. (1981) *Chem. Rev. 81*, 431−444.

Chmielewska, J., Ranby, M., & Wiman, B. (1988) *Biochem. J. 251*, 327−332.

Dano, K., Andreasen, P. A., Grondahl Hansen, J., Kristensen, P., Nielsen, L. S., & Skriver, L. (1985) *Adv. Cancer Res. 44*, 139−226.

Dawes, J., James, K., & Lane, D. A. (1994) *Biochemistry 33*, 4375−4383.

de Agostini, A., Patston, P. A., Marottoli, V., Carrel, S., Harpel, P. C., & Schapira, M. (1988) *J. Clin. Invest. 82*, 700−705.

DeClerck, P. J., De Mol, M., Alessi, M. C., Baudner, S., Paques, E. P., Preissner, K. T., Muller Berghaus, G., & Collen, D. (1988) *J. Biol. Chem. 263*, 15454−15461.

Dewey, T. G. (1991) *Biophysical and Biochemical Aspects of Fluorescence Spectroscopy*, Plenum Press, New York.

Ehrlich, H. J., Keijer, J., Preissner, K. T., Gebbink, R. K., & Pannekoek, H. (1991) *Biochemistry 30*, 1021−1028.

Gettins, P., Patston, P. A., & Schapira, M. (1993) *Bioessays 15*, 461−467.

Hekman, C. M., & Loskutoff, D. J. (1985) *J. Biol. Chem. 260*, 11581−11587.

Huber, R., & Carrell, R. W. (1989) *Biochemistry 28*, 8951−8966.

Karolin, J., Johansson, L. B.-Å., Strandberg, L., & Ny, T. (1994) *J. Am. Chem. Soc. 116*, 7801−7806.

Kinosita, K., Jr., Kawato, S., & Ikegami, A. (1977) *Biophys. J. 20*, 289.

Lawrence, D., Strandberg, L., Grundstrom, T., & Ny, T. (1989) *Eur. J. Biochem. 186*, 532−533.

Lawrence, D. A., Strandberg, L., Ericson, J., & Ny, T. (1990) *J. Biol. Chem. 265*, 20293−20301.

Levin, E. G., & Santell, L. (1987) *Blood 70*, 1090−1098.

Loskutoff, D. J., van Mourik, J. A., Erickson, L. A., & Lawrence, D. (1983) *Proc. Natl. Acad. Sci. U.S.A. 80*, 2956−2960.

Matheson, N. R., van Halbeek, H., & Travis, J. (1991) *J. Biol. Chem. 266*, 13489−13491.

Mimuro, J., & Loskutoff, D. J. (1989) *J. Biol. Chem. 264*, 936−939.

Mimuro, J., Schleef, R. R., & Loskutoff, D. J. (1987) *Blood 70*, 721−728.

Moscatelli, D., & Rifkin, D. B. (1988) *Biochim. Biophys. Acta 948*, 67−85.

Mottonen, J., Strand, A., Symersky, J., Sweet, R. M., Danley, D. E., Geoghegan, K. F., Gerard, R. D., & Goldsmith, E. J. (1992) *Nature 355*, 270−273.

Munch, M., Heegaard, C., Jensen, P. H., & Andreasen, P. A. (1991) *FEBS Lett. 295*, 102−106.

Ny, T., Sawdey, M., Lawrence, D., Millan, J. L., & Loskutoff, D. J. (1986) *Proc. Natl. Acad. Sci. U.S.A. 83*, 6776−6780.

Rosenberg, R. D., & Damus, P. S. (1973) *J. Biol. Chem. 248*, 6490−6505.

Saksela, O. (1985) *Biochim. Biophys. Acta 823*, 35−65.

Saksela, O., & Rifkin, D. B. (1988) *Annu. Rev. Cell Biol. 4*, 93−126.

Sherman, P. M., Lawrence, D. A., Yang, A. Y., Vandenberg, E. T., Paielli, D., Olson, S. T., Shore, J. D., & Ginsburg, D. (1992) *J. Biol. Chem. 267*, 7588−7595.

Shieh, B.-H., Potempa, J., & Travis, J. (1989) *J. Biol. Chem. 264*, 13420−13423.

Shore, D. J., Day, D. E., Francis-Chmura, A. M., Verhamme, I., Kvassman, J., Lawrence, D. A., & Ginsberg, D. (1995) *J. Biol. Chem. 270*, 5395−5398.

Strandberg, L., Lawrence, D. A., Johansson, L. B.-Å., & Ny, T. (1991) *J. Biol. Chem. 266*, 13852−13858.

Strandberg, L., Karolin, J., Johansson, L. B.-Å., Fa, M., Aleshkov, S., & Ny, T. (1994) *Thromb. Res. 76*, 253−267.

Szabo, A. (1984) *J. Chem. Phys. 81*, 150−167.

Urano, T., Strandberg, L., Johansson, L. B.-Å., & Ny, T. (1992) *Eur. J. Biochem. 209*, 985−992.

Wiman, B., Almquist, A., Sigurdardottir, O., & Lindahl, T. (1988) *FEBS Lett. 242*, 125−128.

Wun, T. C., Palmier, M. O., Siegel, N. R., & Smith, C. E. (1989) *J. Biol. Chem. 264*, 7862−7868.

York, J. D., Li, P., & Gardell, S. J. (1991) *J. Biol. Chem. 266*, 8495−8500.

BI951294H